

Lattice relaxation, electronic screening, and spin and orbital phase diagram of LaTiO₃/SrTiO₃ superlattices

Satoshi Okamoto,^{1,*} Andrew J. Millis,¹ and Nicola A. Spaldin²

¹*Department of Physics, Columbia University, 538 West 120th Street, New York, New York 10027, USA*

²*Materials Research Laboratory and Materials Department, University of California, Santa Barbara, California, 93106, USA*

(Dated: January 22, 2019)

The effects of lattice relaxation in LaTiO₃/SrTiO₃ superlattices are investigated using a combination of LDA+*U* density functional theory, and Hartree-Fock effective Hamiltonian calculations. We find noticeable (~ 0.1 – 0.2 Å) distortions of the TiO₆ octahedra in the near-La region. The resulting screening changes the Ti *d*-electron density substantially. Tight-binding fits to the relaxed-lattice band structure, combined with Hartree-Fock calculations of the resulting model, reveal a novel phase with *xy* orbital order, which does not occur in bulk LaTiO₃, or in the hypothetical unrelaxed structure.

PACS numbers: 73.20.-r,73.21.Cd,75.70.-i

Recent advances in the techniques of pulsed laser deposition and molecular beam epitaxy have allowed the creation of “oxide heterostructures” consisting of alternating layers (of arbitrary number of unit cells) of different transition metal oxide compounds. The physics becomes particularly interesting when one or more of the constituent layers is a compound with correlated electron properties [1, 2] such as Mott insulating behavior, high temperature superconductivity or colossal magnetoresistance. In addition to advances in fabrication, recent years have seen tremendous progress in the characterization [3, 4, 5, 6, 7, 8, 9, 10, 11, 12, 13] and theoretical analysis [14, 15, 16, 17, 18, 19] of such structures. However, before this work, the crucial issue of lattice relaxation has not been systematically addressed.

We expect the lattice relaxation issue to be important because a key feature of heterostructures is “charge redistribution” [4]; that is the redistribution of electrons from one layer to another, and consequent changes from the bulk valence values, driven by the difference in electrochemical potentials between the component materials. Simple estimates and tight-binding model studies suggest that the resulting dipole layer involves a charge density of about $\frac{1}{2}e$ /unit cell, displaced by one to two lattice constants [14]. The electric field associated with such a dipole layer is not small, ~ 0.1 eV/Å, and may be expected to drive significant changes in atomic positions compared with the bulk materials. Further, many experimentally relevant heterostructures involve ferroelectric or nearly ferroelectric materials, for example SrTiO₃, for which enhanced dielectric response is an issue.

The purpose of this paper is to calculate the magnitude and nature of the lattice relaxation in LaTiO₃/SrTiO₃ heterostructures, and to determine its effect on the electronic properties. First, we calculate the relaxed structures of [LaTiO₃]_{*n*}[SrTiO₃]_{*m*} superlattices using the LDA+*U* method of density functional theory within the projector augmented wave (PAW) approach [20] as im-

plemented in the *Vienna Ab initio Simulation Package* (VASP) [21, 22]. We consider [001] (*n-m*) superlattices in which a unit consisting of *m* planes of LaTiO₃ followed by *n* planes of SrTiO₃ layers is repeated in the [001] (*z*) direction, similar to those studied experimentally by Ohtomo *et al.* [4]. Technical details include the rotationally invariant LDA+*U* method of Liechtenstein *et al.* [23] with *U* = 5 and *J* = 0.64 eV for the Ti *d* states [24]. In addition, if we treat the La *f* states within the LDA, we find that the empty La *f* bands lie only ~ 2 eV above the Fermi level, leading to a spurious mixing and level repulsion with the Ti-derived *d* bands. Since in practice, the La *f* bands should lie much higher in energy [25], we impose a large *U* of 11 eV, and *J* = 0.68 eV on the La *f* states. Omitting the La *f* *U* changes the results, for example reducing the lattice distortions by ≈ 50 %. For Sr and Ti, we use PAW potentials in which semi-core *s* states are treated as valence states, (Sr_{*sv*} and Ti_{*sv*} in the VASP distribution) while for La and O, we use standard potentials (La and O in the VASP distribution), and we use a $4 \times 4 \times 1$ *k*-point grid and an energy cutoff 500 eV. The lattice constants *a* and *b* are fixed to the experimental value for cubic SrTiO₃ (3.91 Å) which is the substrate used in the experiments [4]. The *c* axis lattice constant and atomic *z* coordinates are adjusted, while retaining the tetragonal symmetry of the crystal, until the forces on the ions are less than 0.01 eV/Å.

Figure 1 shows our calculated relaxed lattice structures for two representative cases: (1-8) and (2-7) heterostructures. The largest structural relaxations occur in the TiO₂ layer at the LaTiO₃-SrTiO₃ interface (Ti_{0.5} in the upper panel and Ti₁ in the lower panel) with the Ti displaced from its ideal position by 0.15 Å in the (1-8) case and 0.18 Å in the (2-7) structure. As a consequence, the lengths of the Ti-Ti distances across the LaO planes (Ti_{-0.5}-Ti_{0.5} and Ti₀-Ti_{±1}) are approximately 2 % larger than those across SrO planes. This “ferroelectric-like” distortion produces a local ionic dipole moment which

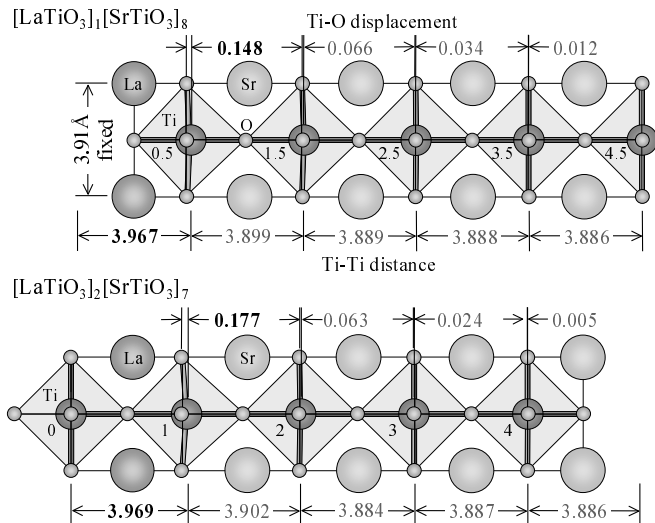


FIG. 1: Calculated optimized lattice structures of superlattices $[\text{LaTiO}_3]_1[\text{SrTiO}_3]_8$ (upper figure) and $[\text{LaTiO}_3]_2[\text{SrTiO}_3]_7$ (lower figure); half of the unit cell is shown in each case. The optimized z axis lattice constants are $c = 35.09 \text{ \AA}$ and 35.17 \AA for $[\text{LaTiO}_3]_1[\text{SrTiO}_3]_8$ and $[\text{LaTiO}_3]_2[\text{SrTiO}_3]_7$, respectively. The intertitanium distances (lower lines) and displacements of the Ti ions relative to the O_2 planes (upper lines) are also indicated. The center of the LaTiO_3 region is taken as the zero of the z coordinate in each case and the Ti ions are labeled by their relative z positions.

screens the Coulomb field created by the substitution of Sr^{2+} by La^{3+} ions. Moving further away from the interface, the magnitude of the ferroelectric-like distortion decays rapidly, while the Ti-Ti distance reverts to a constant value very close to that in bulk SrTiO_3 .

An important quantity for physical insight and more detailed theoretical analysis is the spatially resolved conduction band charge density: loosely speaking, the Ti d occupancy. To obtain this, we make use of the fact that the ground state within $\text{LDA}+U$ is a highly polarized ferromagnetic state in which the magnetization density can be ascribed to the conduction bands. Following Ref. [26], we compute a smoothed magnetization density $\bar{m}(z)$, shown as the light gray line in Fig. 2, by planar averaging and smoothing in z over a range $\pm a/2$. We identify the integral of $\bar{m}(z)$ over a unit cell with the conduction-band charge density in that cell. The total (summed over all cells) conduction-band charge obtained in this way is within $\sim 1\%$ of the expected 1 electron per La ion in the two-layer heterostructure, but only ~ 0.85 electrons per La in the one-layer structure probably because the one-layer structure is not fully spin-polarized. Therefore in the latter case we renormalize the density appropriately.

Fig. 2 compares our calculated Ti d charge densities for relaxed (black squares) and unrelaxed (white squares) lattices for $[\text{LaTiO}_3]_1[\text{SrTiO}_3]_8$ (upper panel)

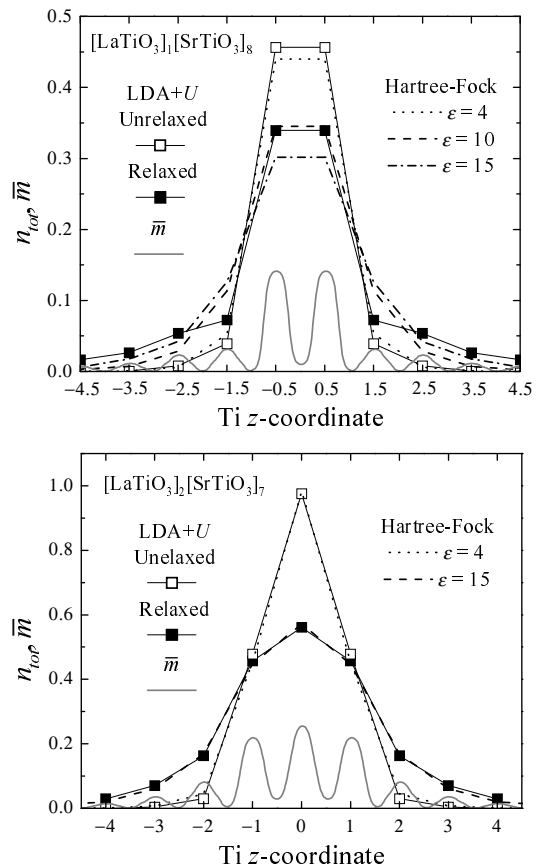


FIG. 2: Charge and magnetization densities for (1-8) and (2-7) heterostructures. Filled and open squares: conduction band charge densities per unit cell, relaxed and unrelaxed superlattices, respectively, obtained as described in text. Light lines: smoothed magnetization densities of relaxed heterostructures. Dotted, broken, and dash-dot lines: results of model Hartree-Fock calculation with realistic band parameters for unrelaxed and relaxed structures. $U = 5$ and $J = 0.64 \text{ eV}$, and dielectric constant ϵ indicated.

and $[\text{LaTiO}_3]_2[\text{SrTiO}_3]_7$ (lower panel). In both superlattices, the screening provided by lattice relaxation reduces the charge density on the central Ti layer and produces a long “tail” in the charge distribution, extending far away from the interface. The effect is particularly large in the two-layer structure, reducing the middle-layer density by almost a factor of two. We note that in each case the interface layer ($\text{Ti}_{0.5}$ or Ti_1) remains electronically well defined, with the density dropping by approximately 0.3 electrons between the Ti at the interface, and its neighbor surrounded by two SrO layers. The relaxed-lattice charge densities agree within experimental uncertainties with the Ti^{3+} values measured by Ohtomo *et al.*[4], both in terms of peak values (experiment: 0.3 in one-layer and 0.4 in two-layer) and of the slow decay away from the central region.

In addition to changing the charge-density profile, as shown in Fig. 2, the changes in interatomic distances as-

sociated with the lattice relaxation lead to changes in the orbital overlaps. To address the effect of these changes in electronic structure on the many-body physics, we use the LDA+ U results to derive a tight-binding model, which we solve in the Hartree-Fock approximation, computing relaxed and unrelaxed heterostructures. The form of the tight-binding model is discussed in Ref. [14]. It has three classes of parameters: the electronic structure, parameterized by level splittings and hoppings, which we obtain by fitting to our LDA+ U calculations, “Kanamori” multiplet interactions, which we treat as adjustable parameters, and the screening of the long-ranged Coulomb interaction, which we parameterize by a dielectric constant ε chosen to approximately reproduce the charge densities of Fig. 2.

Following previous work [14], we represent the electronic structure by a tight-binding model involving three orbitals labeled $\alpha = xy, xz, yz$ representing three t_{2g} -symmetry Ti-O antibonding bands, with on-site energies ε_α and nearest-neighbor hopping t_α^δ along $\delta = x, y, z$ directions given by the usual Slater-Koster rules. (further-neighbor hoppings are factors of 5-10 smaller) The electronic-structure Hamiltonian is $H_{el} = \sum_l [H_{\parallel}(z_l) + H_{\perp}(z_l)]$ with

$$H_{\parallel}(z_l) = \sum_{\alpha, \vec{k}_{\parallel}} \left[-2t_\alpha^x(z_l) \cos k_x - 2t_\alpha^y(z_l) \cos k_y + \varepsilon_\alpha(z_l) \right] \times d_{\alpha\vec{k}_{\parallel}}^\dagger(z_l) d_{\alpha\vec{k}_{\parallel}}(z_l), \quad (1)$$

$$H_{\perp}(z_l) = \sum_{\alpha, \vec{k}_{\parallel}} \left[-t_\alpha^z(z_l) d_{\alpha\vec{k}_{\parallel}}^\dagger(z_l) d_{\alpha\vec{k}_{\parallel}}(z_l + 1) + H.c. \right]. \quad (2)$$

The heterostructures shown in Fig. 1 have too many bands for a direct tight-binding analysis to be practical. We observe that there are three kinds of Ti site in the heterostructures (those surrounded by La, surrounded by Sr, or with two La and two Sr neighbors), and correspondingly three types of Ti-Ti bonds. Since the hopping parameters depend on the Ti environment, we obtain them by fitting bands obtained from LDA+ U calculations for simplified two-layer heterostructures with atomic positions fixed to those found in the full (1-8 and 2-7) structures. Hopping parameters between different kinds of Ti along z direction in the heterostructures are estimated considering the fact that the hoppings are in fact “second order” processes via O p state. During these additional band structure calculations, we eliminate the on-site Coulomb interaction for Ti d states which may cause an additional level splitting among d states, while the on-site Coulomb interaction for La f states is preserved.

Representative values for t_α^δ and ε_α are given in table I. We see that the largest effect of the relaxations is a decrease in the hoppings for d_{xz} and d_{yz} orbitals at the interface layers, and that the larger distortions in the two-layer heterostructure lead to larger effects. De-

TABLE I: Tight-binding parameters for symmetry-inequivalent hoppings in units of eV derived by fits to LDA+ U band calculations of simplified heterostructures with atomic positions taken from LDA+ U calculations of relaxed and unrelaxed [LaTiO₃]₁[SrTiO₃]₈ (labeled 1) and [LaTiO₃]₂[SrTiO₃]₇ (labeled 2) heterostructures. Parameters of relaxed (R) and unrelaxed (U) heterostructures are shown in upper and lower lines, respectively. For larger z_l , $t_{xy}^{x,y} = t_{xz}^{x,z} = t_{yz}^{y,z} = 0.5$ eV and $\varepsilon_{xy,xz,yz} = 0$.

	$t_{xy}^{x,y}$	t_{xz}^x	t_{xz}^z	ε_{xy}	ε_{xz}
z_l	- 0.5	- 0.5	-0.5 0.5	- 0.5	- 0.5
1 R	- 0.53	- 0.46	0.44 0.57	- 0.23	- 0.19
1 U	- 0.55	- 0.55	0.56 0.51	- 0.27	- 0.36
z_l	0 1	0 1	0 1	0 1	0 1
2 R	0.63 0.53	0.63 0.38	0.47 0.58	0.66 0.06	0.66 -0.07
2 U	0.63 0.55	0.63 0.55	0.59 0.51	0.66 0.27	0.66 0.36

crease in the in-plane hoppings for d_{xz} and d_{yz} is as large as ≈ 30 % in the (2-7) heterostructure and that in the z -direction hoppings is ≈ 20 % in both the (1-8) and (2-7) heterostructures. Similarly, a moderate level splitting (~ 0.13 eV) occurs in the transition layer.

To extract appropriate values for the dielectric constant, ε , we add the long-ranged Coulomb terms to the tight-binding model (for details see Ref. [14]), and adjust ε to fit the LDA+ U charge densities, as shown in Fig. 2. One sees that the results for the unrelaxed case are well described by a ε of 4, and that the effects of screening from the lattice relaxations can be simulated reasonably well (but not perfectly) by increasing the dielectric constant to ≈ 15 . The main deficiency is that the dielectric constant model overestimates the rate at which charge density decays far from the heterostructure, in the $n \lesssim 0.05$ region, for the (1-8) heterostructure (cf. upper panel). We associate this with the nonlinear screening characteristic of nearly ferroelectric materials.

Finally, to investigate the changes due to the lattice relaxations, we compute the many-body phase diagrams for the relaxed and unrelaxed cases using the band parameters derived above and the methods of Ref. [14]. To avoid complexity coming from the interference between different La regions we use isolated heterostructures in which n LaTiO₃ layers were sandwiched by a semi-infinite number of SrTiO₃ layers. Figure 3 compares our phase diagrams for relaxed and unrelaxed heterostructures.

First we comment on features that are common to both relaxed and unrelaxed cases. The present calculations are an improvement over previously published [14] Hartree-Fock calculations in that they allow for the possibility of a fully alternating (both within plane and from plane to plane) antiferro-orbital ordering state. We denote this phase as OO-G, and see that it is in fact the ground state over wide regions of the phase diagram in both cases. This phase is favored by strong correlations (large U) and

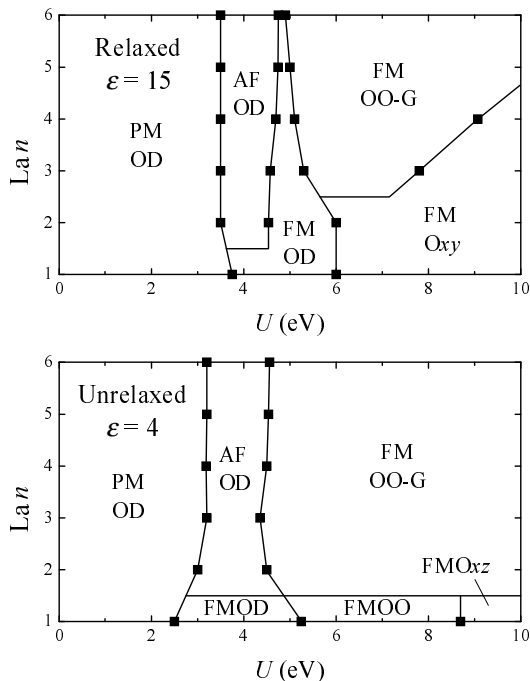


FIG. 3: Spin and orbital phase diagrams of realistic three-band model heterostructures as a function of the intraorbital Coulomb interaction U with interorbital Coulomb interaction $U' = U - 2J$ and exchange interaction $J = 0.6$ eV and La layer thickness n computed within the Hartree-Fock approximation. Upper panel: relaxed structure with $\epsilon = 15$ and appropriate band parameters obtained from LDA+ U , lower panel: unrelaxed structure with $\epsilon = 4$. PM: paramagnetic, FM: ferromagnetic states, AF: antiferromagnetic state in which the magnetic moment alternates from plane to plane, OD: orbitally disordered state, OO-G: orbitally ordered state in which xz and yz orbitals alternate in x, y and z directions, $Oxy(xz)$: orbitally ordered state in which xy (xz or yz) occupancy is predominant, and OO: orbitally ordered state in which xz and yz orbitals alternate in z direction.

electron densities near one [24]. In thicker heterostructures, at the edge of the high density region, we expect this phase to be replaced by a ferro-orbital phase for reasons similar to those discussed in Ref. [28]; this will be discussed in detail elsewhere [29].

The most striking *differences* between the phase diagrams result from the different density profiles. In particular the lower central-layer charge density and wider transition regions of the relaxed structure shift the phase boundaries to higher U values, and disfavor the OO-G phase. The lattice relaxation also changes the local environment at each Ti site, but in the calculations presented here these effects cannot be isolated from the larger effects due to changes in screening. Insight into the importance of the symmetry breaking at fixed screening is gained by comparing Fig. 3 to our previously published Fig. 1 of Ref. [14]-1 and Fig. 2 of Ref. [14]-1. These figures show a phase diagram corresponding to similar

charge densities, but with isotropic hoppings and no level splitting. Note that when the previous figure was constructed, only calculations with in-plane translation invariance were possible, the OO-G phase could not be studied and a higher energy layered orbital state ($xz-yz$) was found at all thicknesses. We see that the effect of the symmetry breaking, larger hopping intensities for d_{xy} band, is to replace this phase by the ferro-orbital Oxy for small n . We note that the Oxy phase is not observed in the unrelaxed case at $n = 1$, even with the symmetry-broken hopping parameters because, in the unrelaxed $n = 1$ case, the central Ti layer ($Ti_{\pm 0.5}$) density is too high. Instead, the system prefers other orbitally ordered states with narrower xy -plane band widths.

To summarize, we have performed first-principles calculation on $LaTiO_3/SrTiO_3$ superlattices and investigated the effect of lattice relaxation on the charge screening and change in the model parameters. Our primary observation is a large polar distortion of TiO_6 octahedra at the near La region in which Ti and O ions are displaced, leading to screening which reduces the central layer charge density, substantially consistent with experiment [4] and disfavoring staggered orbital orderings. In addition, for thin heterostructures at strong correlation, the symmetry breaking due to the distortion favors a novel uniform orbital ordering Oxy not found in bulk.

We thank A. M. Rappe, C. Ederer and D. R. Hamann for helpful discussions. S.O. acknowledges the Materials Research Laboratory, UC Santa Barbara for hospitality. This research was supported by the DOE under Grant No. ER 46169 (A.M. and S.O.), by the NSF under grant number CHE-0434567 (N.S.), and made use of MRL Central Facilities supported by the MRSEC Program of the National Science Foundation under award No. DMR05-20415.

* Electronic address: okapon@phys.columbia.edu

- [1] M. Imada, A. Fujimori, and Y. Tokura, Rev. Mod. Phys. **70**, 1039 (1998).
- [2] Y. Tokura and N. Nagaosa, Science **288**, 462 (2000).
- [3] M. Izumi, Y. Ogimoto, Y. Konishi, T. Manako, M. Kawasaki, and Y. Tokura, Mat. Sci. Eng. B **84**, 53 (2001) and references therein.
- [4] A. Ohtomo, D. A. Muller, J. L. Grazul, and H. Y. Hwang, Nature (London) **419**, 378 (2002).
- [5] S. Gariglio, C. H. Ahn, D. Matthey, and J.-M. Triscone, Phys. Rev. Lett. **88**, 067002 (2002).
- [6] I. Bozovic, G. Logvenov, M. A. J. Verhoeven, P. Caputo, E. Goldobin, T. H. Geballe, Nature (London) **422**, 873 (2003); I. Bozovic, G. Logvenov, M. A. J. Verhoeven, P. Caputo, E. Goldobin, and M. R. Beasley, Phys. Rev. Lett. **93**, 157002 (2004).
- [7] H. Yamada, Y. Ogawa, Y. Ishii, H. Sato, M. Kawasaki, H. Akoh, and Y. Tokura, Science **305**, 646 (2004).
- [8] M. Varela, S. D. Findlay, A. R. Lupini, H. M. Christen,

- A. Y. Borisevich, N. Dellby, O. L. Krivanek, P. D. Nellist, M. P. Oxley, L. J. Allen, and S. J. Pennycook, *Phys. Rev. Lett.* **92**, 095502 (2004).
- [9] C. W. Schneider, S. Hembacher, G. Hammerl, R. Held, A. Schmehl, A. Weber, T. Kopp, and J. Mannhart, *Phys. Rev. Lett.* **92**, 257003 (2004).
- [10] V. Peña, Z. Sefrioui, D. Arias, C. Leon, J. Santamaria, J. L. Martinez, S. G. E. te Velthuis, and A. Hoffmann, *Phys. Rev. Lett.* **94**, 057002 (2005).
- [11] J. Stahn, J. Chakhalian, Ch. Niedermayer, J. Hoppler, T. Gutberlet, J. Voigt, F. Treubel, H-U. Habermeier, G. Cristiani, B. Keimer, and C. Bernhard, *Phys. Rev. B* **71**, 140509(R) (2005).
- [12] G. Yu. Logvenov, C. W. Schneider, J. Mannhart, and Yu. S. Barash, *Appl. Phys. Lett.* **86**, 202505 (2005).
- [13] J. J. Kavich, M. P. Warusawithana, J. W. Freeland, P. Ryan, X. Zhai, R. H. Kodama, J. N. Eckstein, [cond-mat/0512158](https://arxiv.org/abs/cond-mat/0512158).
- [14] S. Okamoto and A. J. Millis, *Nature (London)* **428**, 630 (2004); *Phys. Rev. B* **70**, 075101 (2004).
- [15] S. Okamoto and A. J. Millis, *Phys. Rev. B* **70**, 241104(R) (2004).
- [16] S. Okamoto and A. J. Millis, *Phys. Rev. B* **72**, 235108 (2005).
- [17] Z. S. Popovic and S. Satpathy, *Phys. Rev. Lett.* **94**, 176805 (2005).
- [18] J. K. Freericks, *Phys. Rev. B* **70**, 195342 (2004).
- [19] N. Pavlenko and T. Kopp, *Phys. Rev. B* **72**, 174516 (2005).
- [20] P. E. Blochl, *Phys. Rev. B* **50**, 17953 (1994).
- [21] G. Kresse and J. Furthmuller, *Phys. Rev. B* **54**, 11169 (1996).
- [22] G. Kresse and D. Joubert, *Phys. Rev. B* **59**, 1758 (1999).
- [23] A. I. Liechtenstein, V. I. Anisimov and J. Zaanen, *Phys. Rev. B* **52**, R5467 (1995).
- [24] T. Mizokawa and A. Fujimori, *Phys. Rev. B* **51**, R12880 (1995).
- [25] M. T. Czyżyk and G. A. Sawatzky, *Phys. Rev. B* **49**, 14211 (1994).
- [26] N. Sai, A. M. Kolpak, and A. M. Rappe, *Phys. Rev. B* **72**, 020101(R) (2005).
- [27] J. C. Slater and G. F. Koster, *Phys. Rev.* **94**, 1498 (1954).
- [28] C. Lin, S. Okamoto, A. J. Millis (in preparation).
- [29] S. Okamoto, A. J. Millis, and N. A. Spaldin (in preparation).